International Journal of Geology, Earth & Environmental Sciences ISSN: 2277-2081
An Open Access, Online International Journal Available at http://www.cibtech.org/jgee.htm
2025 Vol. 15, pp. 292-312/Kouadio et al.
Research Article

CONTRIBUTION OF SATELLITE IMAGERY TO THE IDENTIFICATION OF METALLOID DEPOSITS : THE CASE OF THE DEPARTMENT OF BOCANDA (CENTRAL-EAST OF CÔTE D'IVOIRE)

Kouadio Fossou Jean Luc Hervé[1]*, Kouamelan Alain Nicaise[1], Adingra Koffi Pohn Martial[1], Ouattara Jacques Kleporon[1], Kouame Kouadio Séverin[1]
[1]Training and Research Unit in Earth Sciences and Mineral Resources, Geology, Mineral and Energy Resources Laboratory, University Félix Houphouët-Boigny, Abidjan Cocody, 22 BP 582 Abidjan 22, Côte d'Ivoire
**Author for Correspondence: fossou.kouadio95@ufhb.edu.ci*

ABSTRACT
The department of Bocanda, located in the N'Zi Comoé region, was the subject of this geological study. The methods used to improve our geological knowledge of the area were remote sensing, petrographic analysis, structural analysis and metallogenic studies. At the remote sensing level, the study identified five lithological units and a linear network whose main orientations were NE-SW, NW-SE and E-W. Petrographic analysis revealed the presence of andesites, granites, metagrauwackes, sericite schists, sericite-chlorite schists, granodiorites and monzonites. Green schist facies metamorphism and hydrothermal alteration of the vein and pervasive types were identified in the area. The vein type is characterised by quartz veins, while the pervasive type is characterised by epidotization, chloritization, sericitization, silicification, and sulfidation. A structural analysis was conducted to identify the types of deformation present in the study area. Two types of deformation were identified: brittle deformation, which is manifested by fractures, faults, dislocations, veins, and fissures, and ductile deformation, which is manifested by foliation, schistosity, swells, C/S fabrics, and mineral stretch lineations. All the structures in the study area are oriented in the NE-SW, NW-SE and E-W directions. Metallogenic results show that the disseminated metalliferous paragenesis is enclosed in metagrauwackes but is controlled by the structure. This paragenesis comprises chalcopyrite, pyrite and haematite.

Keywords **:** *Imaging, Petrography, Structure, Metallogeny, Bocanda, Côte d'Ivoire*

1. INTRODUCTION
Gold mineralisation in West Africa is generally associated with Birimian formations from the Paleoproterozoic era (Milesi *et al.,* 1989). Due to its geological history, Côte d'Ivoire accounts for around 35% of these formations in West Africa. These formations have therefore been the focus of academic and mining research for decades, resulting in the identification of numerous deposits, such as those at Angovia, Agbahou, Hiré, Tongon, Bonikro, Aféma, Lafigué and Iguela (Houssou, 2013 ; Kadio *et al.,* 2010 ; Assié, 2008). The Birimian formations consist of volcanosedimentary grooves or greenstone belts that have been intruded by granitoids (Bessoles, 1977). Gold mineralisation in the Birimian formations is generally associated with shear zones or strike-slip movements (Poulsen *et al.,* 1986). The study area is located in the Comoé Basin in the central-east of Côte d'Ivoire, specifically in the Bocanda department, where geological knowledge is limited due to the lack of detail in the produced geological maps. To overcome this problem, we were asked to consider the area's petrographic, structural and metallogenic characteristics. This will aid the interpretation of future petro-structural and metallogenic data from the Bocanda department, based on satellite, field and laboratory data. The main objective of this work is to improve our understanding of the geological formations in the Bocanda department in terms of their petro-structural and metallogenic characteristics. It will undoubtedly identify a metallotect in the study area to inform mining exploration in the Comoé basin.

2. *Geological Context*

Côte d'Ivoire is located south of the West African craton and within the southern part of the Man Ridge (Bessoles, 1977). Its geology is characterised by a Precambrian basement, which occupies 97.5% of the territory, and a more recent sedimentary cover, which occupies the remaining 2.5% (Tagini, 1971; Figure 1). The Precambrian basement is subdivided into two domains, which are separated by the north-south-trending Sassandra fault (Bessoles, 1977). The western domain is the Archaean or Kenema-Man domain, and the eastern domain is the Proterozoic (Birimian) or Baoulé-Mossi domain. The Archaean domain consists of formations that formed during the Leonian (3.4–2.9 Ga) and Liberian (2.9–2.6 Ga) orogenies (Tagini, 1971). The Leonian orogeny is characterised by four lithological assemblages : grey gneisses, pink granulites, anatexites, ferruginous quartzites, and charnockites (Camil, 1984).

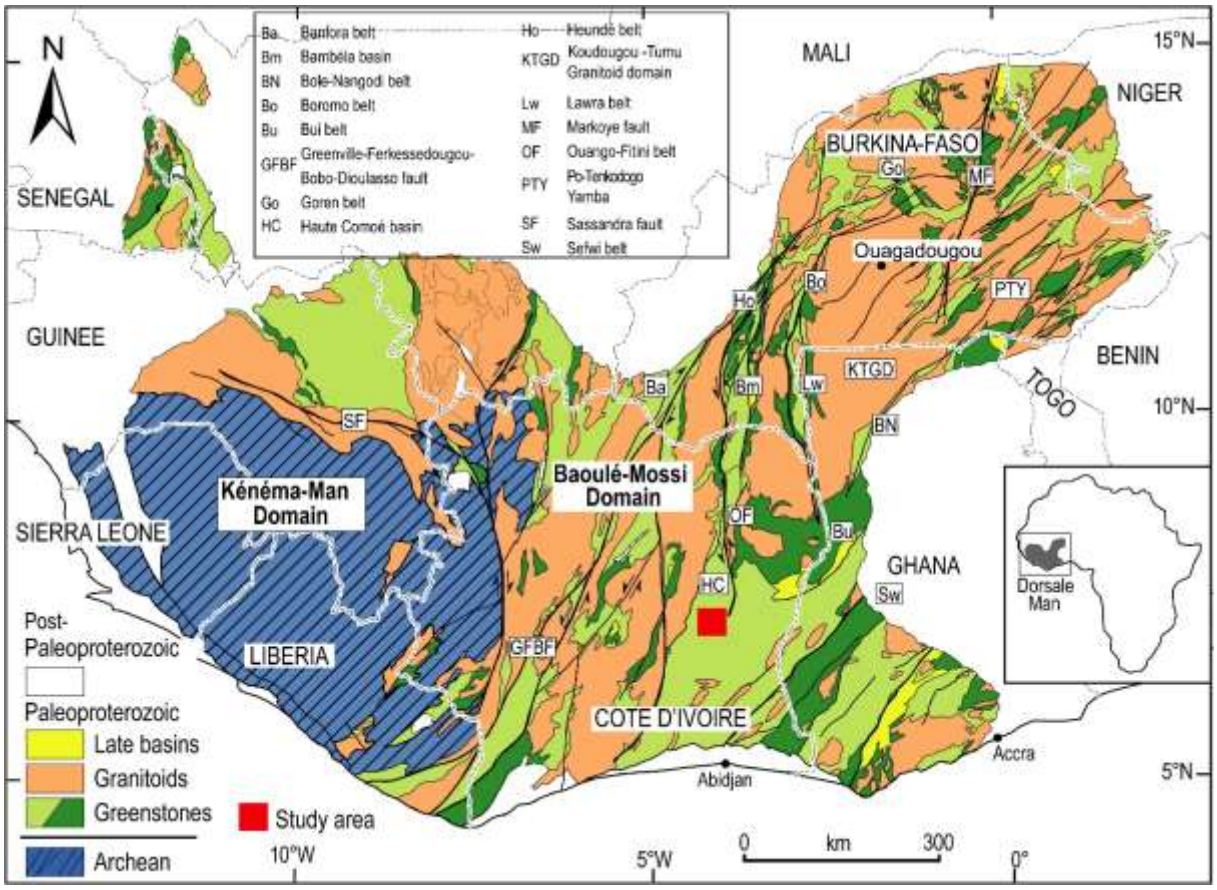

Figure 1: Geological map of the Man Ridge (Baratoux *et al.,* 2011) showing the study area.

The Liberian basement is characterised by granulites, charnockites, migmatites, quartzites and amphibolo-pyroxenites (Camil, 1984). The Proterozoic covers the remainder of the Ivorian basement. Tagini's (1971) work reveals that the Proterozoic formations are structured by the Eburnean megacycle (2,400–1,600 Ma). This is characterised by alternating belts of green rocks and Birimian sedimentary basins oriented NNE–SSW. All of these formations are intruded by several generations of granitoids. Vidal et al. (1996) identified three phases of deformation in the Proterozoic domain of Côte d'Ivoire. According to these authors, the first phase (D1) is characterised by the N-S to NNE-SSW elongation of slightly compressed massifs in an E-W to WNW-ESE direction. Phase D2 is characterised by compression from north-west (NW) to south-east (SE), with straight folds oriented north-east (NE) to north-north-east (NNE). Phase D3 is characterised by NE-SW to N-S shortening, resulting in crenulation schistosity. Our study area is located in the Comoé

Basin, which extends across three countries : Côte d'Ivoire, Ghana and Burkina Faso. The southern part of the basin, in Côte d'Ivoire, consists of Birimian volcanic sedimentary rocks, which occupy more than half of the formations in the area, and granitoids extending over a large area in the far west of the sector (Yao *et al.,* 1995). The results of Ouattara et al. (2012) have indeed highlighted staurolite mica schists and fractures oriented NW-SE intersected by fractures oriented N30° to N40°. The area's rocks are affected by low-grade (green schist) to medium-grade (amphibolite) metamorphism. The geology of the study area comprises sandstone, schist and granitoids. At the structural level, Yao et al. (1990) highlight faults, fold axes and foliations.

3. MATERIALS AND METHODS

3.1 *Satellite imagery data*

Satellite imagery is one of the most effective tools for g eological mapping. Remote sensing techniques can be used to accurately identify geological structures and lineaments (Toutin, 1996). This accuracy makes satellite imagery an indispensable tool for geological mapping. In this study, optical images (Landsat 8 OLI) were used to highlight the different lithological units and associated structures, in order to produce a litho-structural sketch of the study area. The image used in our work was acquired from the USGS website (https://earthexplorer.usgs.gov/). The scene identifier is LC0819605520240203. This indicates that it is a Landsat 8 image of scene 196 and row 55, acquired on 3 February 2024. The downloaded image will undergo pre-processing and processing using ENVI 5.3 and QGIS 3.32.1 software. Pre-processing consists of radiometric correction to eliminate radiometric noise in the different bands, followed by atmospheric correction to eliminate atmospheric noise. The processing consisted of enhancing the image quality in order to identify lithological contrasts and structures. Colour compositions and principal component analyses (PCA) are the different treatments applied to the image to identify lithological facies. Applying gradient filters to the first PCA band enabled us to trace the lineaments of the study area.

3.2 *Macroscopic petrography and structural analysis*

Macroscopic petrography involves locating outcrops and identifying and describing the texture, structure, mineralogical composition, colour, and degree of alteration of rocks. Structural analysis involves identifying geological structures such as foliation, schistosity, banding and faults. The direction, dip and plunge of these structures were measured using a clinometer compass.

3.3 *Microscopic petrography, metallography and microstructural analysis*

Thirteen thin sections and three polished sections were prepared in the workshop of the Laboratory of Geology, Mineral Resources and Energy at Félix Houphouët-Boigny University (UFR-STRM) in Cocody, Abidjan. The petrographic study was conducted using an Euromex optical microscope with transmitted and reflected light, equipped with four magnification lenses (×5, ×20, ×50 and ×100), as well as an image capture device. All of these were connected to a computer. Observations were made in natural and polarised light. This enabled the mineralogical assemblage and metalliferous paragenesis present in the various rocks to be identified.

4. RESULTS

4.1 *Petrographic data*

The geological formations found in the Bocanda department are composed of the following types of rock : andesite, granodiorite, granite, monzonite, metagrauwacke, sericite chlorite schist and sericite schist.

Andesite

Observed in the southern part of the study area, the andesite outcrops in the form of blocks and has a microlitic to microlitic porphyritic texture with a melanocrate colour. Under the microscope, plagioclase minerals are observed in abundance and vary in size from small grains to medium-sized grains. They exhibit polysynthetic twinning. Hornblende is also present in the form of phenocrystals and small crystals. Finally, quartz is present in small proportions in the light grey matrix (Figure 2).

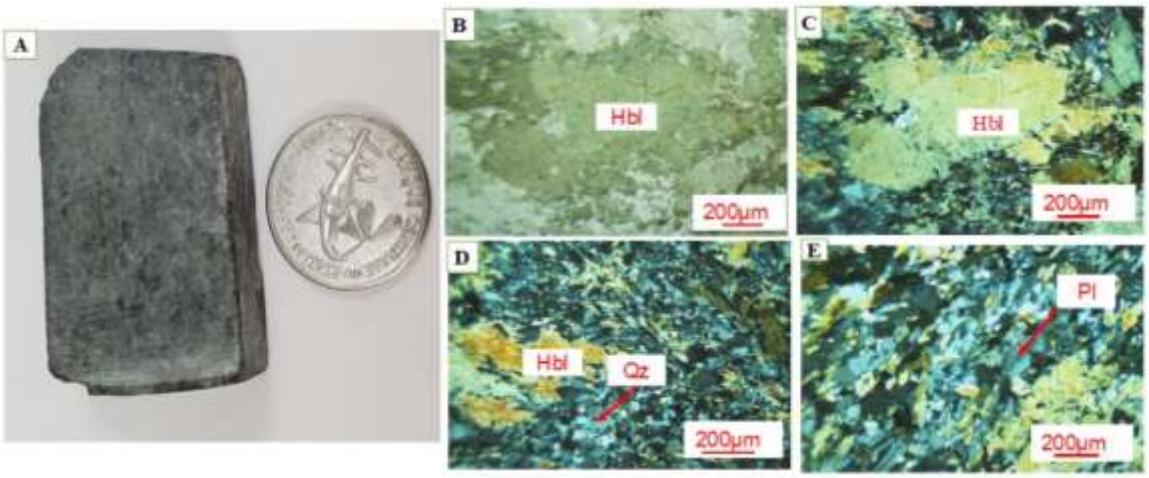

Figure 2 : Macroscopic and microscopic aspects of andesite.
A : Macroscopic appearance ; B–C : Microphotograph of hornblende phenocrystals ; D : Microphotograph of quartz in the matrix ; E : Microphotograph of plagioclase and quartz crystals. Pl : Plagioclase ; Hbl: Hornblende ; Qz: Quartz.

Granodiorite

It has a porphyroid granular texture and a mesocratic colour. Under the microscope, its composition is revealed to be abundant plagioclase in small to large patches characterised by polysynthetic twinning, abundant quartz similar in size to the plagioclase ranging from medium to coarse grain with remarkable rolling extinction, less abundant greenish-brown biotite, and large greenish amphibole crystals (Figure 3).

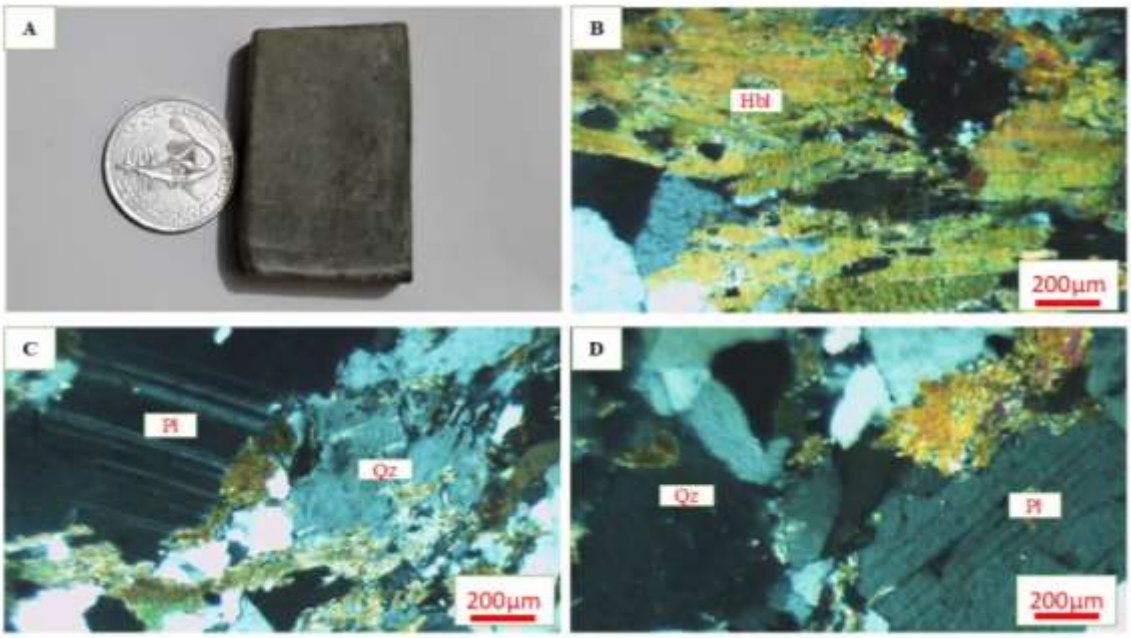

Figure 3 : Macroscopic and microscopic aspects of granodiorite.
A : Macroscopic appearance of granodiorite ; B : Microphotograph of hornblende ; C–D : Microphotographs of plagioclase and quartz phenocrystals. Qz: quartz ; Hbl: hornblende ; Pl : Plagioclase.

Granite

It has a massive appearance and a leucocratic colour. It is located in Akpassanou in Foutou. Under a microscope, it has a granular texture and is composed of xenomorphic quartz the size of the average grain of the rock ; subautomorphic plagioclase with sericite alteration; and biotite, which is less abundant than plagioclase and automorphic in form. It is greenish-brown in colour. Some areas show alteration to epidote. Muscovite and larges areas of xenomorphic microcline are also present. Perthite and myrmekite develop on the plagioclase areas in the form of quartz veinlets. Chlorite is produced by the alteration of biotite. Opaque minerals of xenomorphic form are distributed throughout the rock, and subautomorphic epidote results from the alteration of biotite (Figure 4).

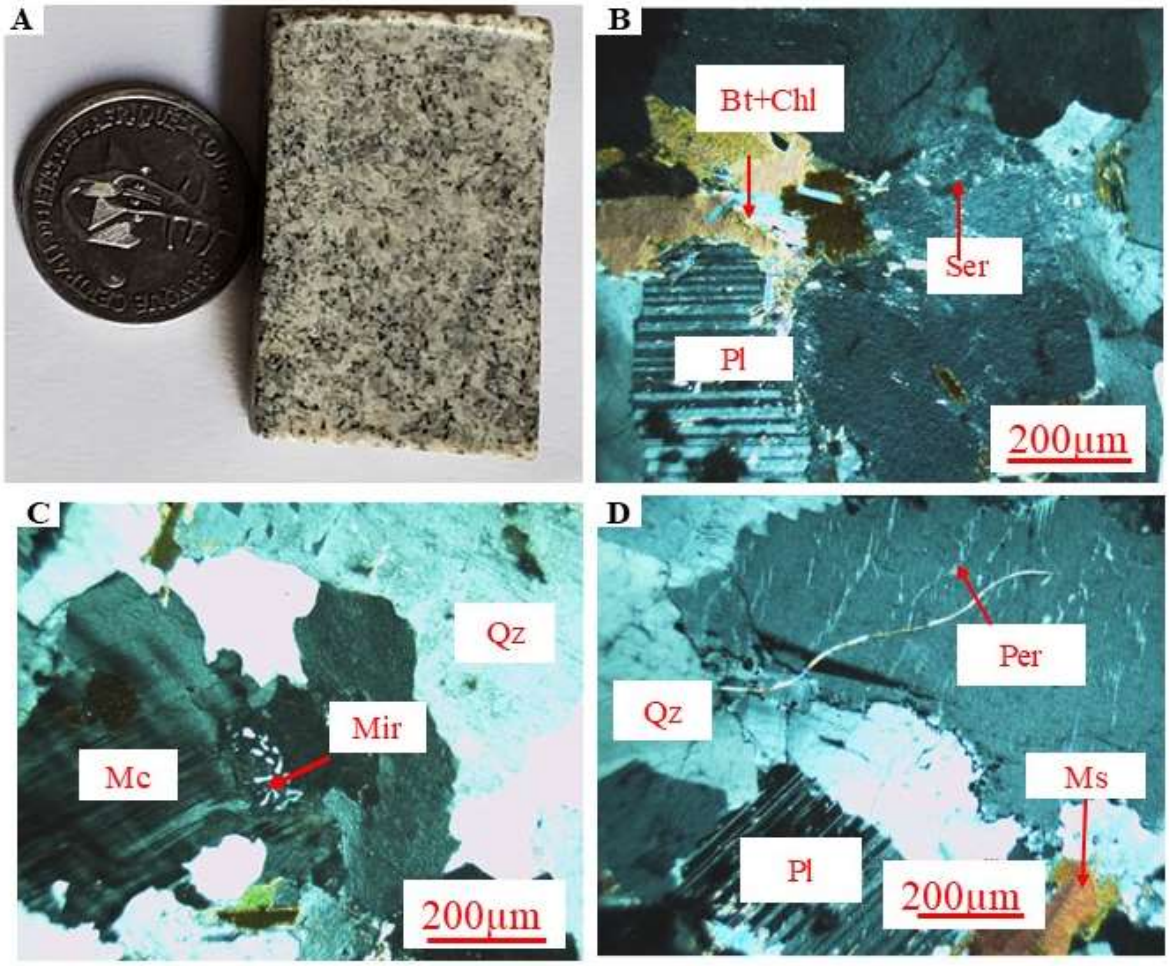

Figure 4 : Macroscopic and microscopic appearance of granite.
A: Macroscopic sample of granite; B : Microphotograph of biotite altered to chlorite; C: Microphotograph of a microcline phenocrystal associated with myrmekites; D: Microphotograph of plagioclase with perthites. Ser: Sericite; Per: Perthite; Bt: Biotite; Chl: Chlorite; Ms: Muscovite ; Mc: Microcline; Qz: Quartz; Mir: Myrmekite; Pl: Plagioclase.

Monzonite

Mesocratic monzonite has been observed in the Foutou area (Figure 5A). Under the microscope, it exhibits a granular texture. It consists of plagioclase crystals ranging in size from small to large, which are characterised by polysynthetic twinning (Figure 5D). Quartz of medium grain size is abundant and xenomorphic with rolling extinction. Orthoclase is characterised by Carlsbad twinning. Minerals such as biotite, hornblende and microcline are less abundant than quartz.

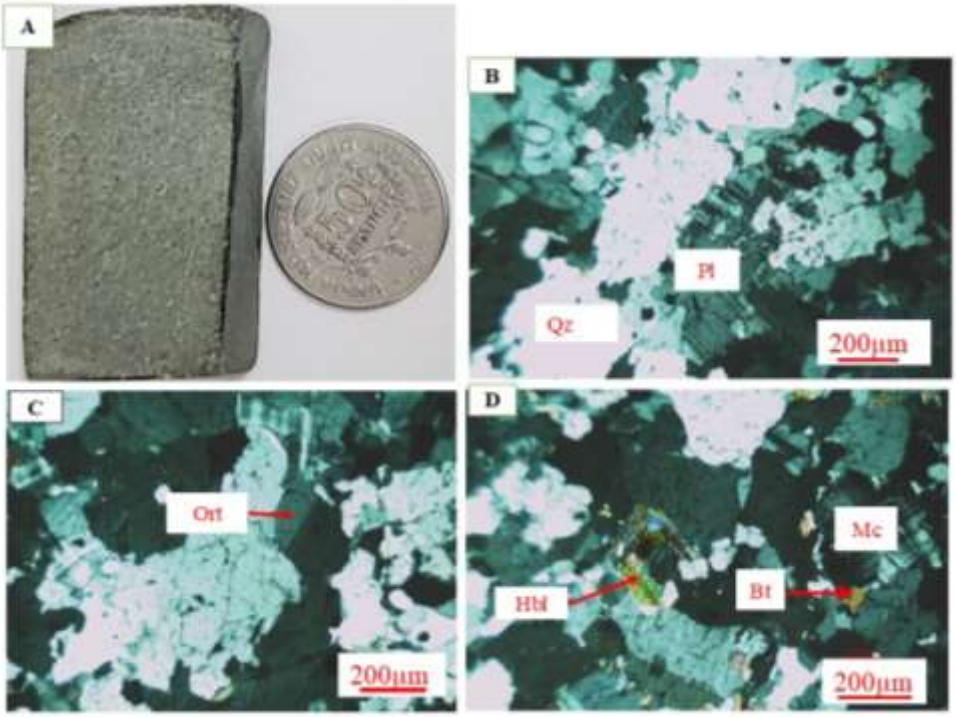

Figure 5 : Macroscopic and microscopic appearance of monzonite.
A: Macroscopic sample of monzonite; B-C-D: Photomicrographs of monzonite.
Pl: Plagioclase; Ort: Orthoclase; Qz: Quartz; Hbl: Hornblende; Bt: Biotite; Mc: Microcline.

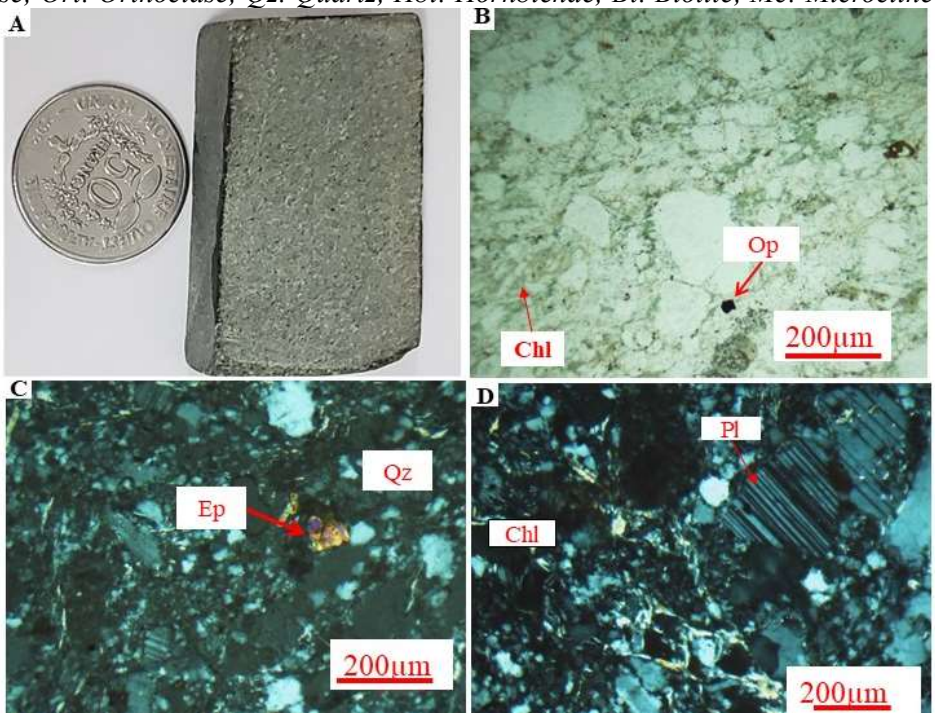

Figure 6 : Macroscopic and microscopic appearance of metagraywacke.
A: Macroscopic appearance of metagraywacke, B: Microphotograph of opaques and chlorite; C-D: Microphotographs of quartz, epidote and plagioclase. Qz: Quartz; Ep: Epidote; Chl: Chlorite; Pl: Plagioclase; Op: Opaques.

Metagraywacke

It is grey in colour and has a granular-lepidoblastic texture (see Figure 6). Under the microscope, quartz and plagioclase porphyroclasts can be seen. This rock is composed of abundant rounded quartz grains with slight relief, and it exhibits remarkable rolling extinction. Plagioclase, which is less abundant than quartz, occurs in the form of small to large minerals, some of which have altered to sericite, chlorite and epidote. Opaque minerals of sub-automorphic to automorphic shape are scattered throughout the rock (Figure 6).

Sericite chlorite schist

This rock appears greenish to the naked eye. Under a microscope, it has a lepidoblastic texture with deformed plagioclase phenocrystals visible. The paragenesis consists of plagioclase that has been altered to sericite. Quartz, which is less abundant than plagioclase, occurs as small to medium-sized grains. Chlorite is distributed throughout the rock in elongated and lamellar forms. The opaque minerals are subautomorphic and occur in clusters (Figure 7).

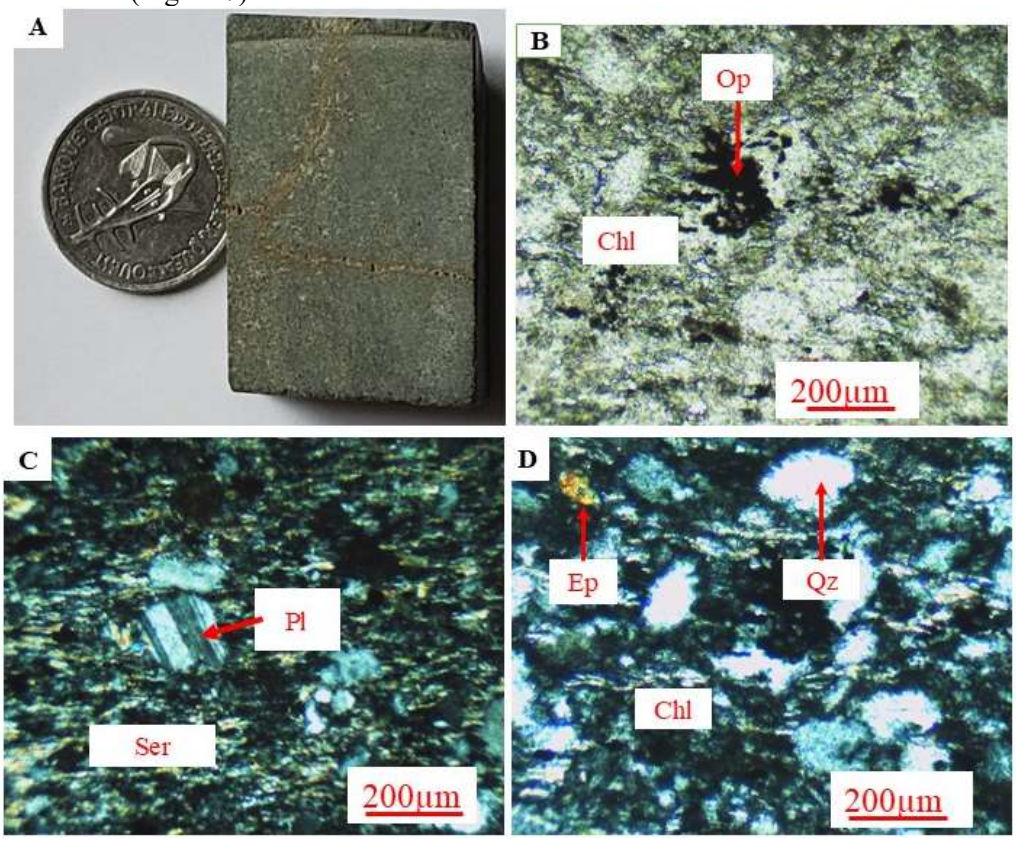

Figure 7 : Macroscopic and microscopic appearance of sericite chlorite schist.
A: Macroscopic appearance of sericite-chlorite schist, B: Microphotograph of chlorite in green and opaque minerals; C: Range of sericite and chlorite; D: Microphotograph of quartz and deformed epidote. Qz: Quartz; Ep: Epidote; Chl: Chlorite; Pl: Plagioclase; Op: Opaques; Ser: Sericite.

4.1.2 *Alterations*

The petrographic study highlights the alteration phenomena that characterise the study area. These are weathering and hydrothermal alteration. Weathering is evident in the form of oxidation traces on geological formations resulting from climatic effects (Figure 8A). There are two types of hydrothermal alteration: vein-type and pervasive. Vein-type alteration is characterised by hydrothermal fluids filling fractures in the rock. This alteration can be observed through the presence of quartz veins of varying thicknesses (Figures 8B–D). Pervasive hydrothermal alteration is characterised by the replacement of the rock's original

minerals. Examples include sericitisation, chloritisation, epidotisation, silicification, and sulphidation (Figure 9).

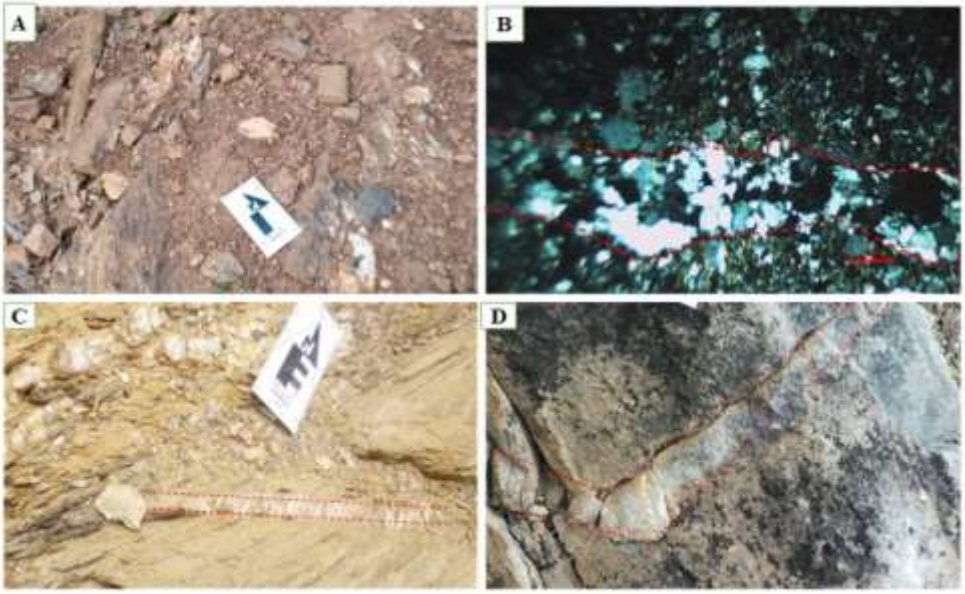

Figure 8 : Weathering and vein alteration.
A: Weathering alteration; B: Microphotograph of a quartz veinlet; C-D: Vein-type alteration of quartz veins at outcrop scale.

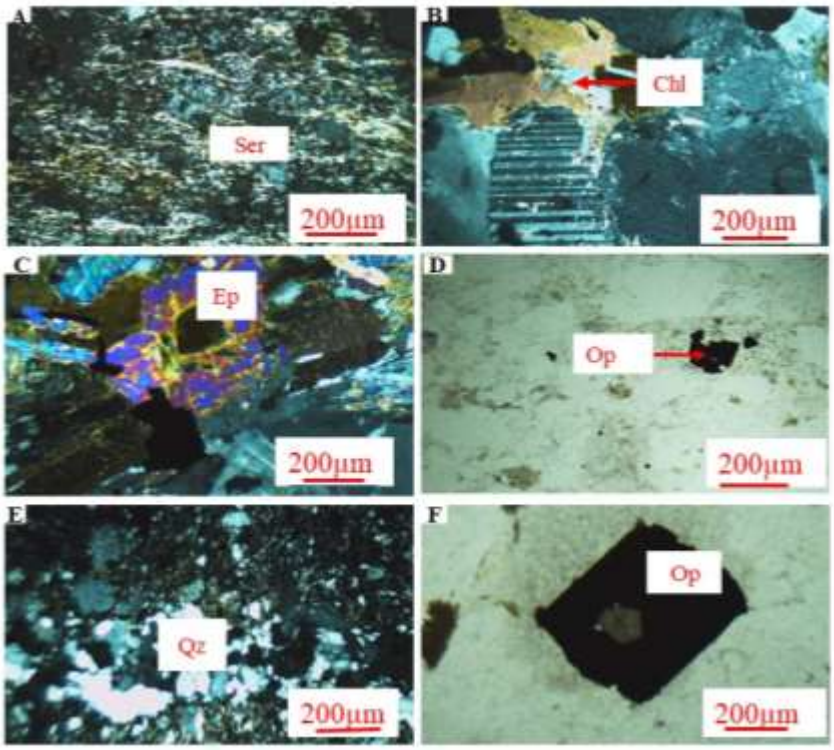

Figure 9 : Pervasive hydrothermal alteration.
A: Microphotograph of sericitisation; B: Microphotograph of chloritisation; C: Microphotograph of epidotisation; E: Quartz vein indicating silicification; D-F: Microphotographs of sulphidation. Qz: Quartz; Op: Opaques; Ep: Epidote; Ser: Sericite; Chl: Chlorite.

4.1.2 *Metallogeny*

The metalliferous paragenesis of the studied area is based on observations of opaque minerals made using a transmitted light optical microscope. The sulphides identified in the area following a metallographic study were mainly chalcopyrite, pyrite and haematite (Figure 10). The study also examined the relationship between metalliferous paragenesis, lithology, deformation and alteration. Microscopic observations reveal that sulphides and oxides are associated with deformed zones. The sulphides observed are disseminated throughout the lithologies. Several mineral associations can be observed. For example, an association of silica, chlorite and chalcopyrite in granites indicates propylitic alteration, whereas an association of quartz, sericite and pyrite indicates phyllic or sericitic alteration.

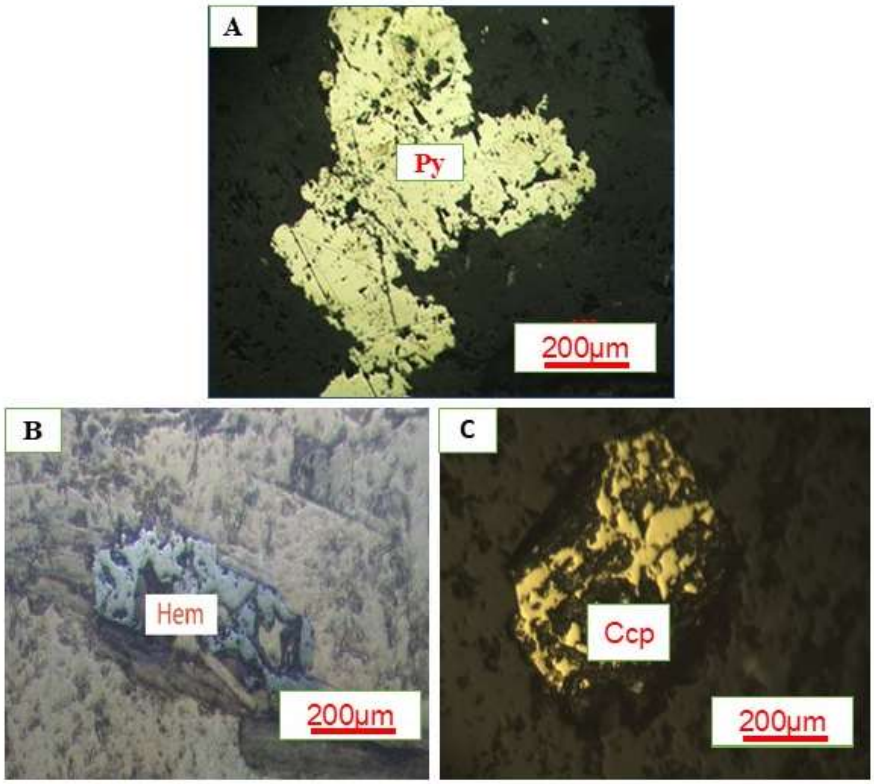

Figure 10 : Microscopic aspects of metalliferous paragenesis.
A: Pyrite in metagraywacke, B: Haematite in granite, C: Chalcopyrite in metagrauwacke. Py: Pyrite, Hem: Haematite, Ccp: Chalcopyrite.

4.2 *Structural data*

4.2.1 *Mesoscopic Structures*

Fractures, veins, faults and dislocations

The observed fractures have orientations ranging from N10° to N160°. Three main directions emerge on the Boua Kouadiokro granites : N76°, N66° and N10° (Figure 11A). The veins observed in the study area are quartz veins (Figure 11B). These veins represent the main structures observed in the study area. Their directions vary between N03° and N135°. Those observed in the Foutou locality have a direction of N115°. Offset structures were observed in several localities, but were particularly evident in Foutou and Apkassanou. Dextral offsets oriented N75° and N35° (Figure 11C) and sinistral offsets oriented N10° (Figure 11D) were indeed observed in Foutou. The directional rosette of the main fractures is NW-SE, N-S and NE-SW (Figure 12A). The directional rosette of the veins throughout the investigated area indicates the following main directions: N-S, NE-SE and NE-SW (Figure 12B).

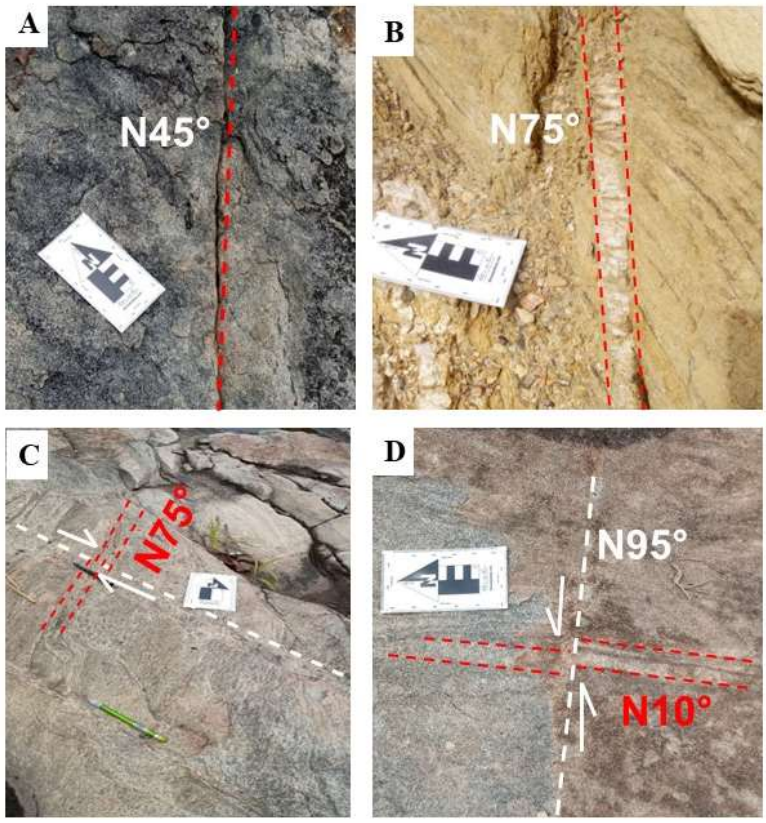

Figure 11 : Photograph of some fragile structures in the Bocanda district.
A: Fractures oriented N45°; B: Quartz vein oriented N75°; C: Dextral offset affecting N75° veins; D: Sinistral offset affects N10° oriented veins.

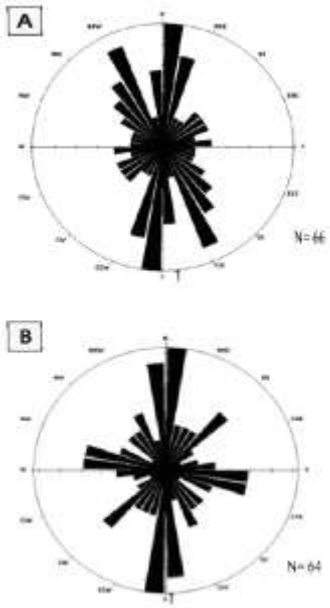

Figure 12 : Directional rosette of main fractures and veins.
A: Fractures; B: Veins.

Foliation, banding, mineral stretching lineation, schistosity

Foliation was observed at several sites. That observed in the Akpassanou locality has a direction of N40° and dips 60° towards the southeast (Figure 13A), while that in Foutou has a direction of N130° and dips 44° towards the northeast. Symmetrical rolls with a direction of N60° were observed in the area's granites (Figure 13B). Stretch lineation is characterised by ferromagnesian minerals stretching in a N80° direction (Figure 13C). Schistosity was observed in the metasediments (Figure 13D) with directions ranging from N80° to N315°. The directional rosette of the foliations indicates a main NE–SW direction (Figure 14A), while the directional rosette of the schistosity indicates WNW–ESE and ENE–WSW directions (Figure 14B).

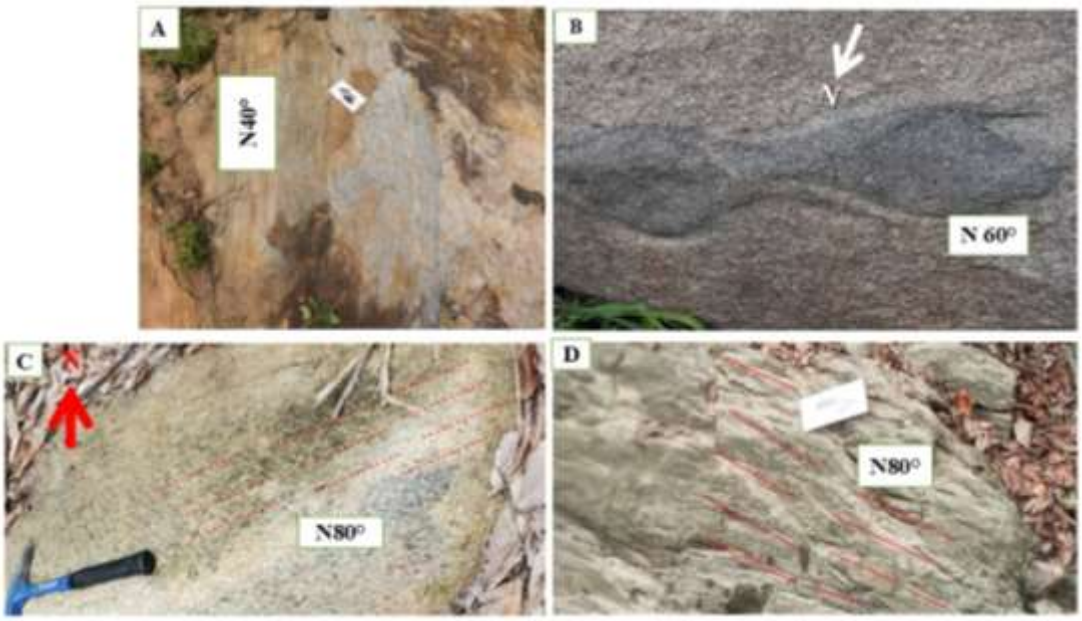

Figure 13 : Photograph of some ductile structures in the Bocanda department.
A: Photograph of foliation oriented N40°; B: Symmetrical rolls oriented N60°; C: Mineral stretching lineation of dark minerals oriented N80°; D: Photograph of schistosity oriented N80°.

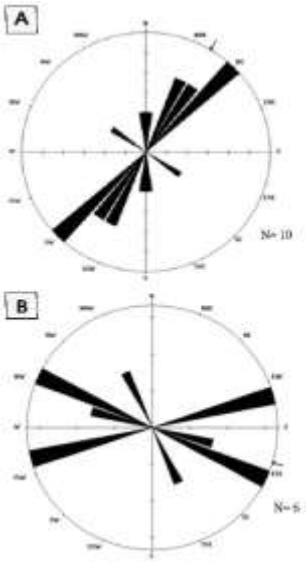

Figure 14 : Directional rosette of foliation and schistosity. *A: Foliation; B: Veins.*

4.2.2 *Microscopic structures*

A large number of structures were observed at a microscopic level. These included C/S fabrics that are characteristic of sinistral shearing, as well as schistosity, stretch lineation, sinistral sigmoid figures, and veinlets (Figure 15).

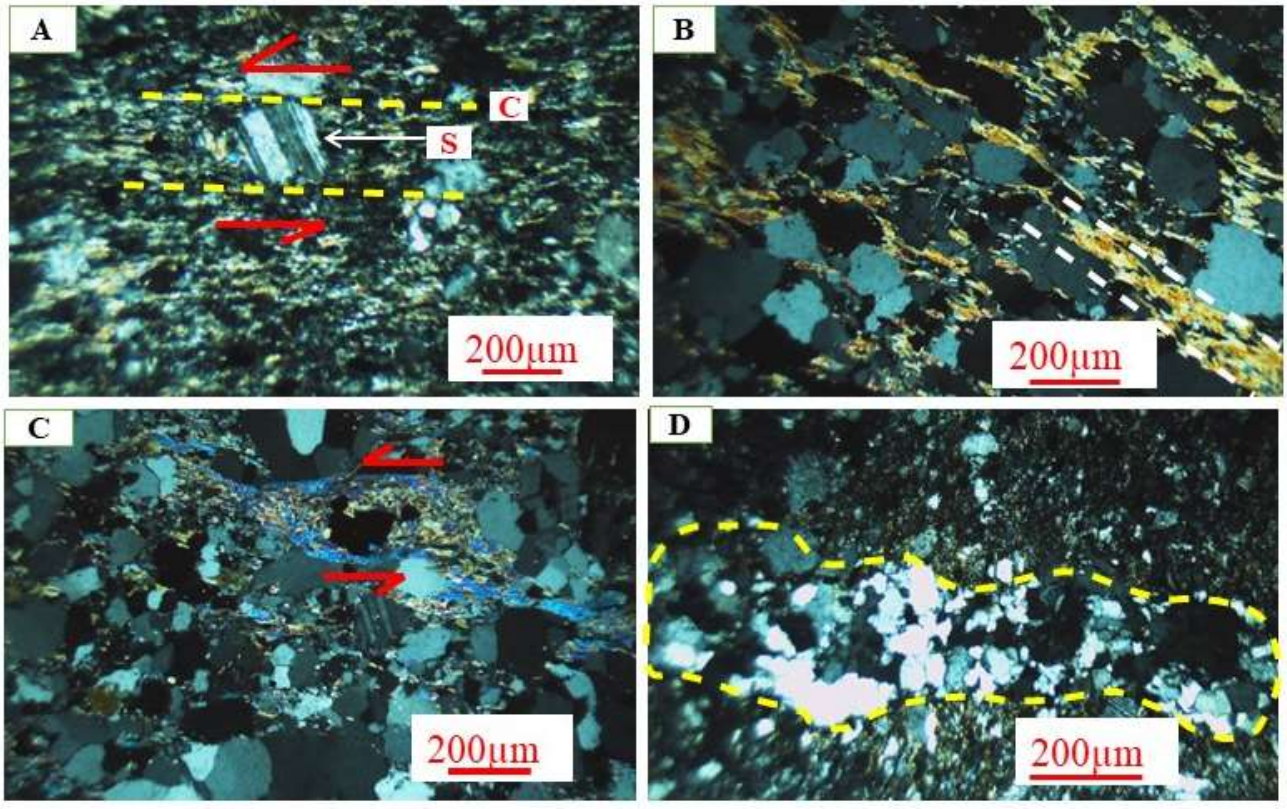

Figure 15 : Microphotograph of structures observed under a microscope.
A: Sinistral C/S fabric; B: Mineral stretching of biotite; C: Sinistral sigmoid figure; D: Quartz vein in a metagrauwacke.

4.3 *Litho-Structural Mapping*

4.3.1 *Lithology map based on Landsat 8 data*

Various treatments were performed on the Landsat 8 image to provide important information about the area's geological features. Radiometric and atmospheric correction, principal component analysis (PCA), band ratios and RGB colour composition of bands 621 enabled five lithologies to be identified (Figure 16). These are designated litho 1, litho 2, litho 3, litho 4 and litho 5. They are yellowish-pink, purple, yellowish-green, greenish-yellow and green, respectively. In terms of dominance, litho 1 is the most prevalent in the investigated area. This is followed by litho 4, litho 2, litho 3, and finally litho 5 which is the least dominant lithology in the study area. Figure 17 shows the resulting lithological map from the digitisation of the RGB colour composition image of bands 621. As identification of the lithologies is subjective, they will be validated following a petrographic study of the field data.

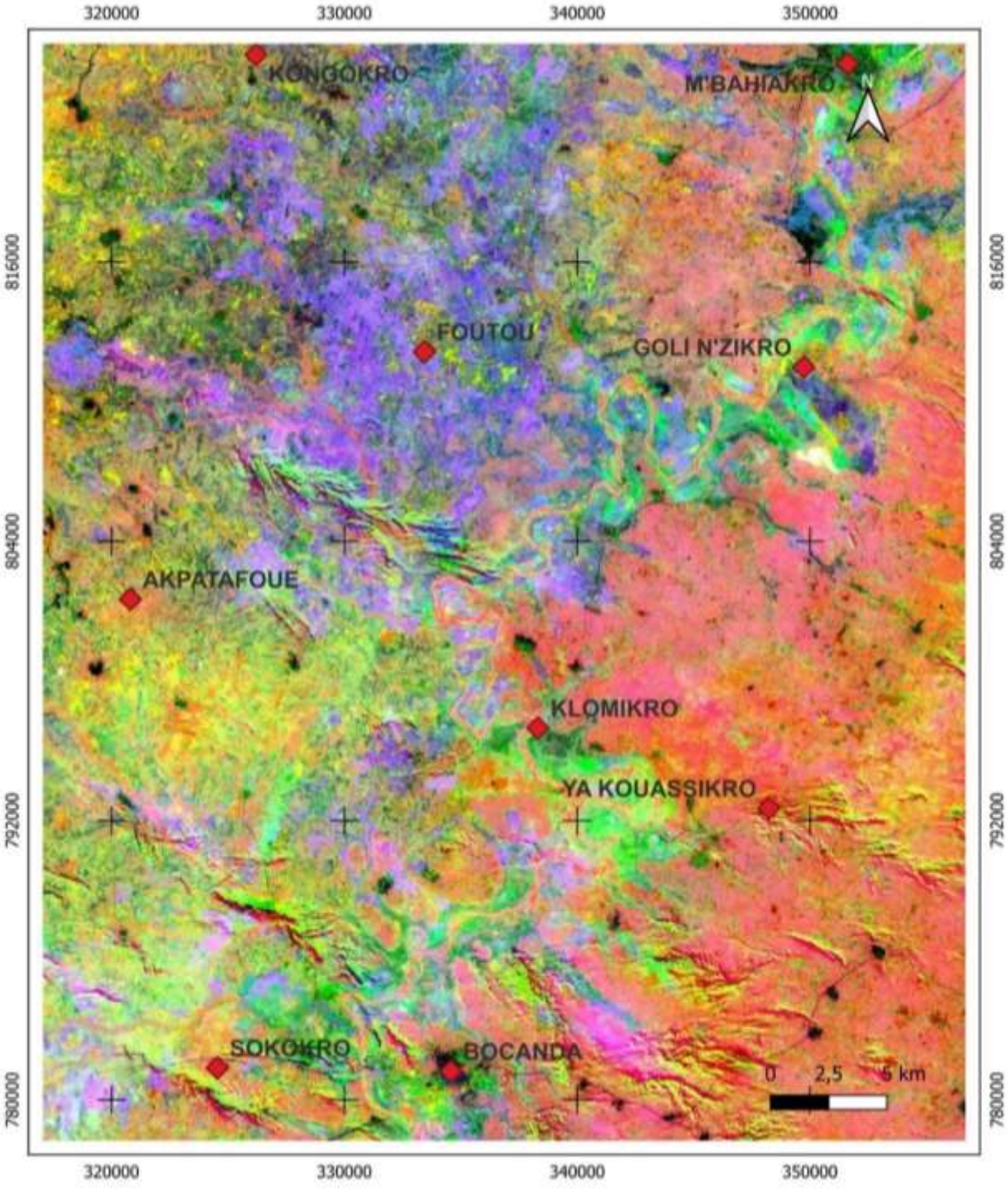

Figure 16 : Image of the RGB colour composition of bands 621.

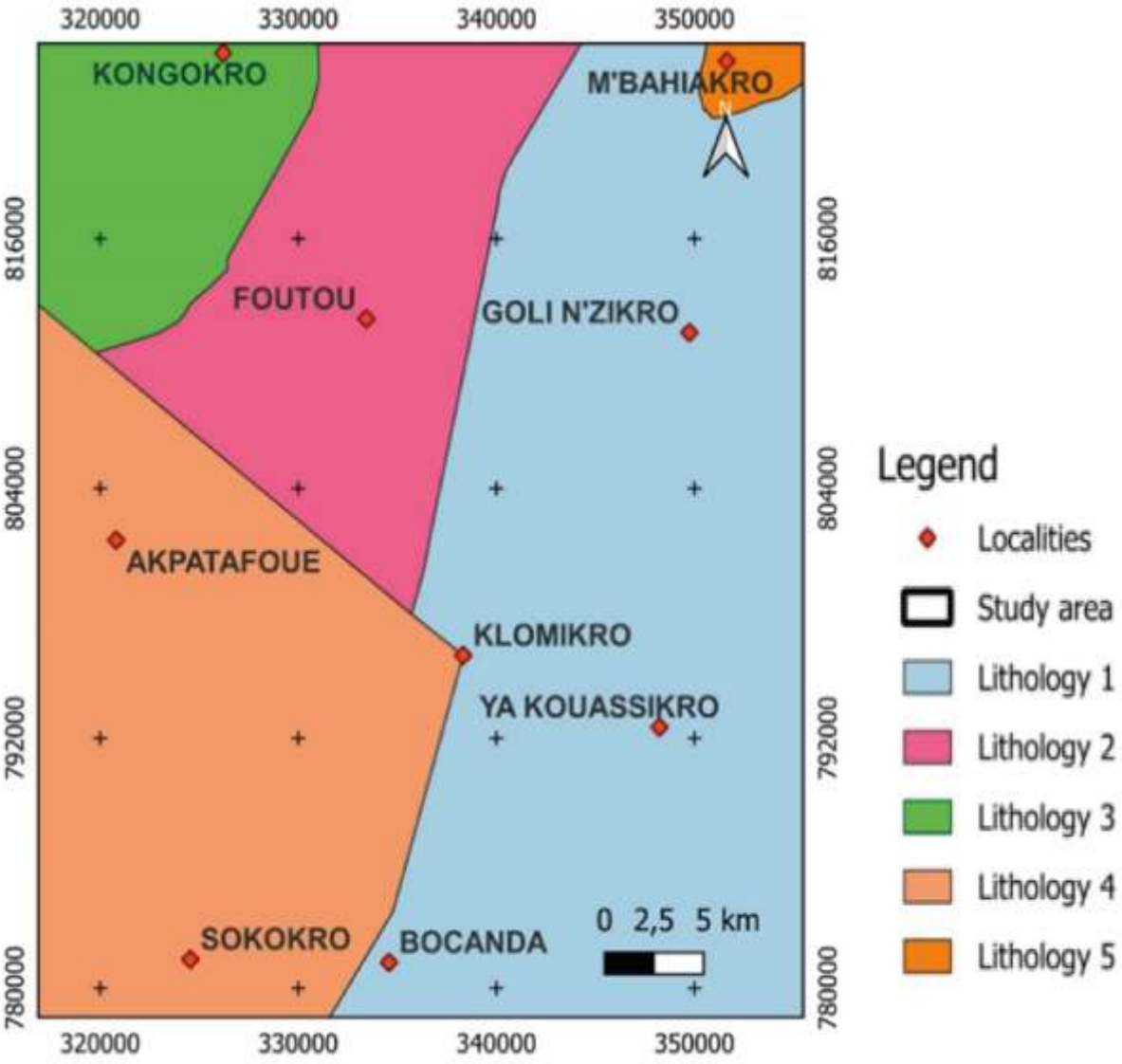

Figure 17 : Lithological sketch of the study area derived from Landsat 8 image processing.

4.3.2 *Map of lineaments*

Processing the lineaments previously traced on figure 18 in ENVI revealed 326 lineaments oriented in several directions (Figure 19A). These lineaments represent the main geological structures, such as fractures, foliations, schistosity, faults, veins and shear zones, as well as the lithological contacts observed in the study area. Analysis of these lineaments using GEOrient software revealed several orientations, primarily NE-SW, NW-SE, and E-W (Figure 19B). The lineaments are unevenly distributed throughout the area, with varying orientations. Fieldwork carried out in the area reveals that the NE–SW lineaments correspond to fractures, dextral faults, foliations, and veins; the NW–SE lineaments correspond to stretch lineations, rolls, schistosity, veins, and sinistral faults. The E–W lineaments correspond to veins.

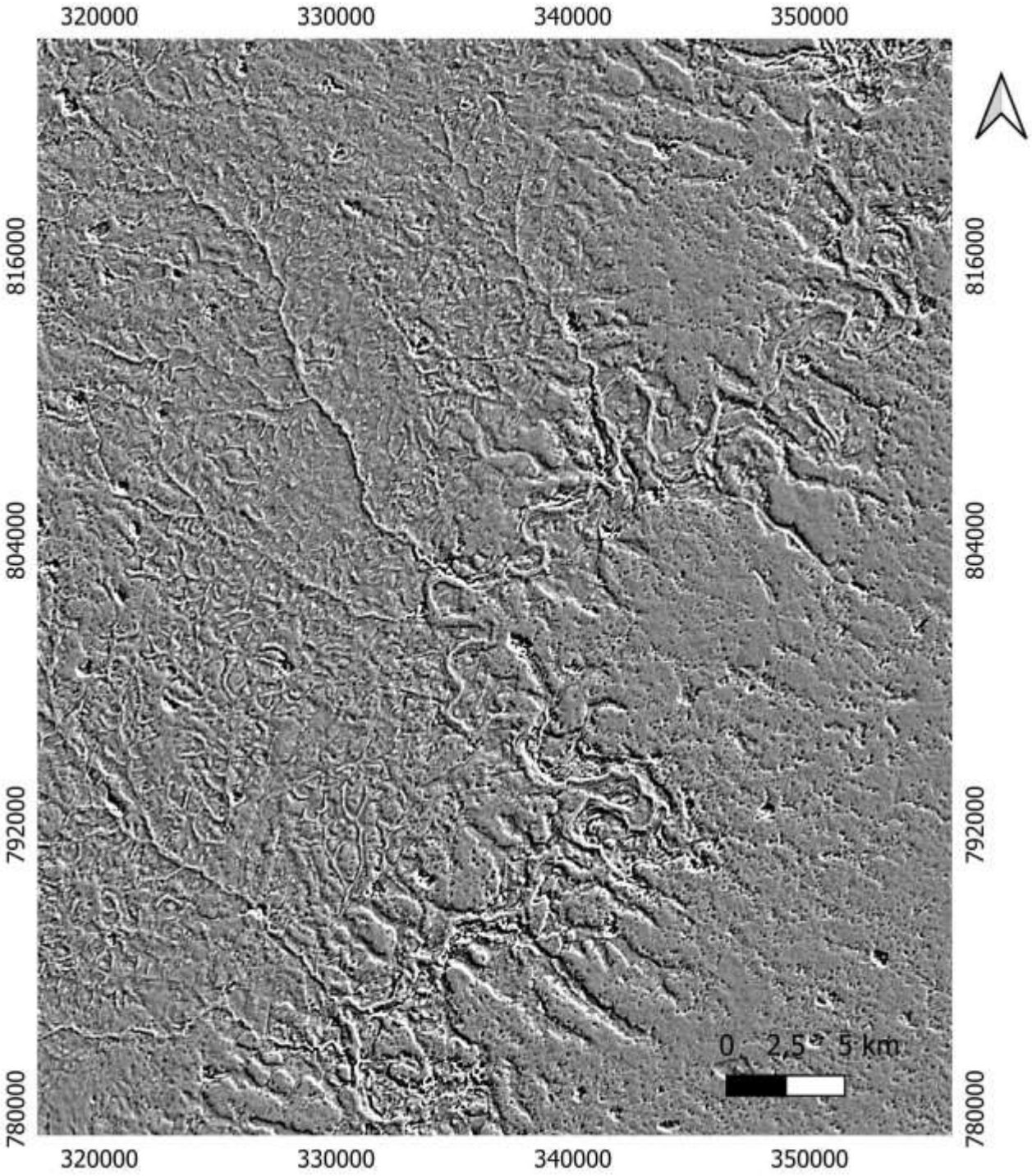

Figure 18 : Result of applying gradient filters to the first band of the PCA.

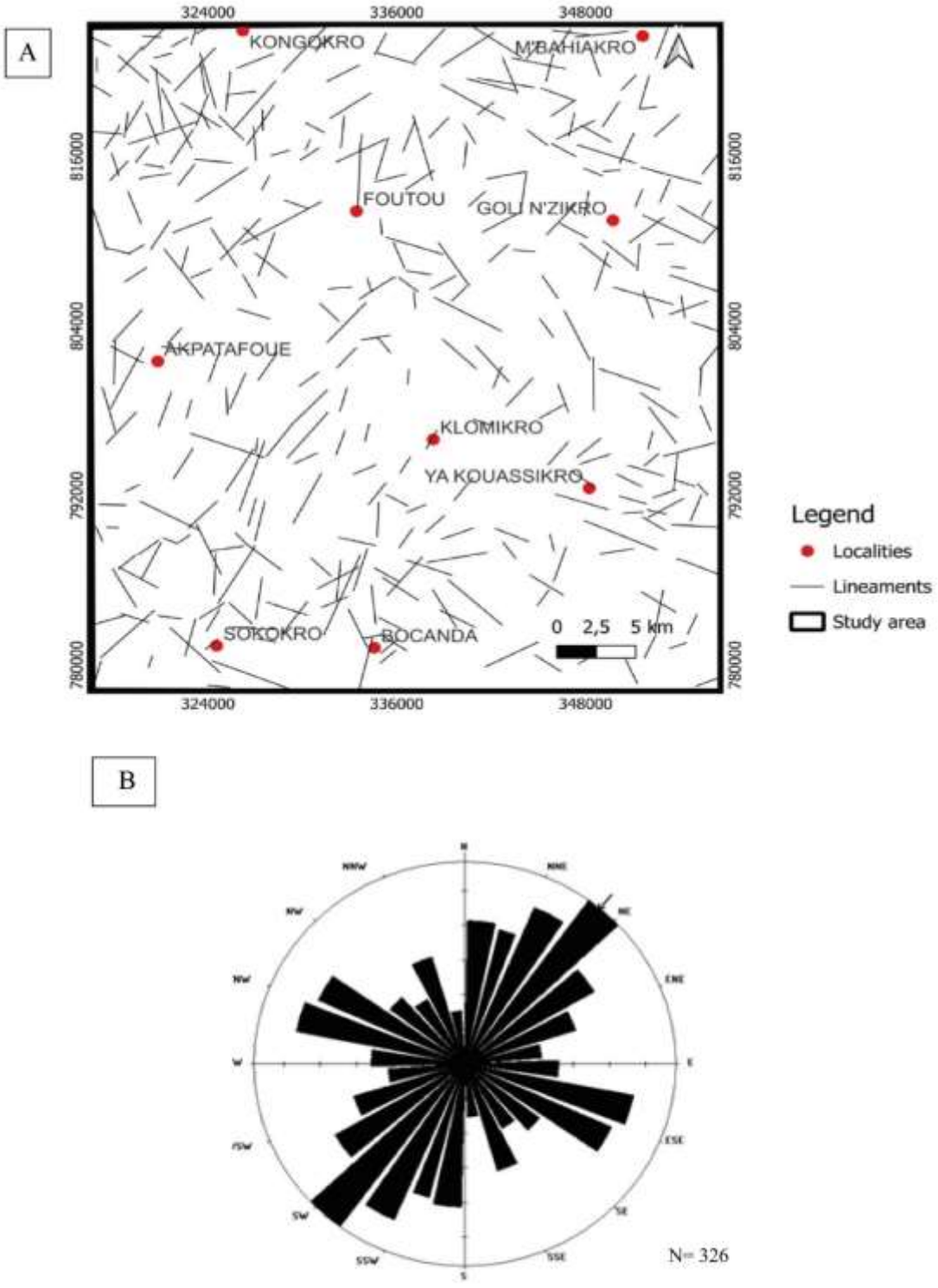

Figure 19 : Map of lineaments (A) associated with the directional rosette (B) of the study area.

In chronological order, the lineaments oriented NE-SW are the oldest, followed by those oriented NW-SE. The E-W lineaments are the most recent. Synthesising remote analytical results, previous work and field results has enabled us to propose a litho-structural sketch (Figure 20). On this sketch, the structures are generally oriented NE-SW and NW-SE. The most significant formations are metasediments, which are located to the east of the study area.

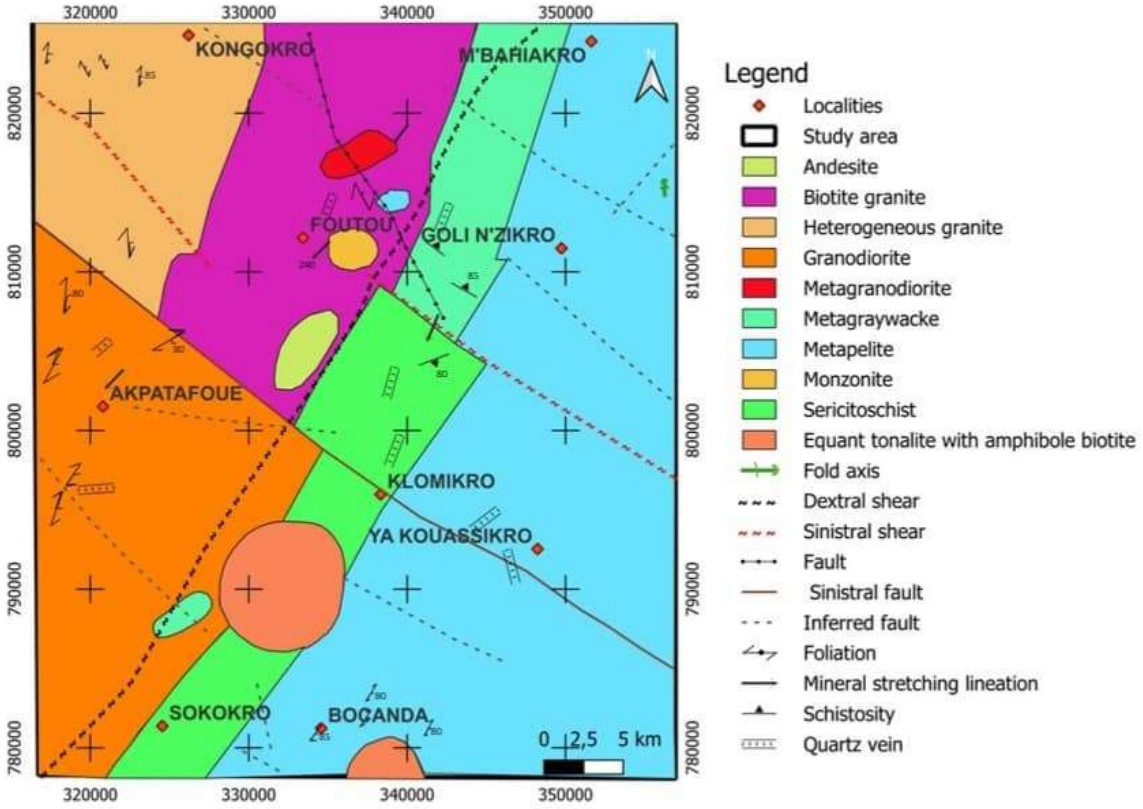

Figure 20 : Litho-structural synthesis sketch of the study area.

5. DISCUSSION

5.1 *In terms of petrography*

The observed lithologies are primarily igneous rocks, such as andesite, granodiorite, monzonite and granite, as well as metasediments, including metagrauwackes, sericitochloritoschist and sericitoschist. The two-mica granites found in the study area mainly consist of quartz, plagioclase, biotite and muscovite. These results are consistent with those reported by Ouattara (1998) in Ferkessédougou and by Gnanzou (2014) in the Dabakala department. Indeed, Gnanzou's work reveals granites with a granular texture, which often contain porphyries. The observed granodiorite consists of plagioclase, quartz, biotite and amphibole. However, this mineralogical composition differs from that described by Adjobi (2021) in the PR807 and PR809 permits in Vavoua, due to the presence of myrmekite. The monzonite observed is identical to that described by Boya et al. (2022) in the Koun Fao department. The observed metasediments are mainly composed of quartz, plagioclase, sericite, chlorite and epidote, which is identical to the composition observed by Boya et al. (2022) in the Koun-Fao department. These results also align with those of Perrouty et al. (2012) in Ghana and Gnanzou (2014) in Dabakala. While the current findings are comparable to those of various other researchers, they diverge from the schists documented by Téha (2019) in the southwestern Comoé basin, with the exception of andalusite. Adingra's (2020) work reveals schists in the south-east of

the Comoé basin that differ from those described in the area due to the presence of garnet and sillimanite minerals. The present study also identified an andesite consisting of plagioclase, hornblende and quartz crystals. This andesite is similar to that observed by Coulibaly (2018) in the south of the Toumodi-Fêtêkro furrow, but differs from that described by Gnanzou (2014).

In terms of metamorphism, the presence of sericite, epidote and chlorite in various geological formations indicates low-grade metamorphism (green schist facies) has occurred. This assertion is supported by Houssou's (2013) work in the Agbahou deposit. Coulibaly's (2018) work in the southern part of the Toumodi-Fètèkro belt is similar to the study area in terms of the metamorphism that affected the region. Regarding alteration minerals (chloritisation, epidotisation, sericitisation, silicification and sulphidation), the results are comparable to Assié's (2008) findings at the Aféma gold prospect.

5.2 ***At the structural level***

All of the geological formations in the study area have been affected by various deformations. These include ductile deformations such as foliation, schistosity, rolling, C/S structures and mineral stretch lineations, as well as brittle deformations such as fractures, quartz veins, pegmatite veins and faults. Most of these deformations correspond to the directions of the Birimian formations. According to Passchier and Trouw (1998), these results suggest the presence of a shear corridor. Furthermore, Sonnendrucker (1967) states that the presence of schistosity, mineral stretch lineations, veins, quartz veins, swells, fractures and faults in an area would indicate a significant deposit. All of the structures in the Bocanda department have the following main directions: NE-SW, NW-SE and E-W. Similar structural directions have also been highlighted by some authors, including Yao (1998), Niamké et al. (2008), Koita et al. (2010), N'Go et al. (2010) and Ouattara et al. (2012) in the N'Zi-Comoé region. These structures all indicate polyphasic deformation in the study area. Vidal et al. (1996) describe Phase D1 as N-S elongation. This manifests as N-S-oriented foliation. Phase D2 is characterised by NE-SE compression, forming foliations oriented between N40° and N60°, schistosity between N70° and N80°, and rolls oriented between N60° and N70°. Phase D3 is characterised by NE-SW to N-S deformation, establishing schistosity of N135° and foliations of N130°. Phase D2 is recognised as an important phase in West Africa by several authors. These include Kouadio (2017) in Côte d'Ivoire, Baratoux et al. (2011) in Burkina Faso and Perrouty et al. (2012) in Ghana. It is believed that this phase is responsible for the formation of shear corridors. Kouadio (2017) identified a late D4 phase in south-western Côte d'Ivoire, where it is evident in numerous fracture networks oriented between N10° and N135°.

5.3 ***In terms of metallogeny***

This study provides information on the metalliferous paragenesis in the study area. These are disseminated in the lithologies and are controlled by the structure. The mineralisation consists of pyrite, chalcopyrite and hematite. This mineralisation is similar to that found in several other Birimian formations in West Africa. Assié (2008) and Kouadio et al. (2024) have respectively studied mineralisation in the south-east (Aboisso) and north-east (Gouméré) of Côte d'Ivoire. This mineralisation is found within metasediments and is controlled by structural features. Metalliferous paragenesis has also been described in Ghana (Oberthür *et al.,* 1996) in the Bogoso and Prestea deposits and in Côte d'Ivoire (Gnanzou, 2014) in the Dabakala region, the Aféma deposit (Assié, 2008) and on Gouméré area (Kouadio *et al.,* 2024). The mineralisation in the study area is epigenetic in nature. Several studies have revealed this type of mineralisation. These include the work of Ouattara et al. (2017) at the Dougbafla deposit in Oumé; Gnanzou (2014) at the Bobosso deposit in Dabakala; Houssou (2013) at the Agbahou deposit in Divo; Kadio et al. (2010) at the Afema deposit in Aboisso and Kouadio et al. (2024) on Gouméré area in Côte d'Ivoire. The mineralisation of the geological formations in the Bocanda department is also associated with significant hydrothermal alteration. Coulibaly et al.'s (2008) work on the Angovia deposit in Yaouré, central Côte d'Ivoire, and Gnanzou's (2014) work in the Dabakala department have revealed hydrothermal alteration similar to ours.

6. CONCLUSION

In terms of petrography, the study area in the department of Bocanda shows two-mica granites, biotite granites, granodiorites, monzonites, andesites, metagrauwackes, sericitochloritoschists and sericitoschists. The study area is also characterised by significant hydrothermal alteration, which is evident in the pervasive and vein-type alteration of the geological formations. The metamorphism affecting the geological formations in the Bocanda department is of the green schist facies type. At the structural level, remote sensing and field data revealed brittle and ductile deformations. Brittle structures include fractures, veins, faults and dextral and sinistral thrusts. The ductile structures observed include foliation, rolling, mineral stretching lineation, schistosity, sigmoid figures, and C/S structures. These structures formed during three phases of deformation: the first characterised by NNE-SSW elongation; the second by NW-SE compression and the third by NE-SW deformation. Analysis of the data indicates that the structures are oriented in the NW-SE, NE-SW and E-W directions. All of these structures reveal the presence of a shear corridor. Metallogenically, the mineralisation is structurally controlled. The metalliferous paragenesis consists of chalcopyrite, pyrite and haematite.

7. ACKNOWLEDGEMENTS

This work was carried out as part of a master's degree research project on the Comoé Basin. This project received financial support from the Faculty of Earth Sciences and Mining Resources and Tanga Resources (Pierrick Courdec).

REFERENCES

Adingra PMK (**2020**). Caracterisation petro-structurale et geochimique des formations birimiennes de la partie sud-est du bassin de la comoe (nord d'alépé-sud Est de la côte d'ivoire) : Implication sur l'evolution geodynamique. Thèse de doctorat, Université Felix Houphouet-Boigny, 220 p.

Adjobi V (**2021**). Etude pétro-structurale des formations géologiques des permis PR101 et PR102 de Vavoua (Centre-Ouest de la Côte d'Ivoire). Mémoire de Master, Université Félix Houphouët Boigny, 63 p.

Assié KE (**2008**). Lode gold mineralization in the Paleoproterozoic (Birimian) volcano-sedimentary sequence of Afema gold district, southeastern Côte d'Ivoire. Thèse de doctorat, University of Clausthal, 198 p.

Baratoux L, **Metelka V**, **Naba S**, **Jessell MW**, **Grégoire M, Ganne J** (**2011**). Juvenile Paleoproterozoic crust evolution during the Eburnean orogeny (~2.2–2.0Ga), western Burkina Faso. Precambrian Research, vol. 191, n° 1-2, pp. 18-45. https://doi.org/10.1016/j.precamres.2011.08.010

Bessoles B (**1977**). Géologie de l'Afrique. Le craton Ouest-Africain. Mémoire BRGM, France, 403 p.

Boya TKLD, **Kouadio FJLH**, **Gnanzou A**, **Adingra PMK**, **Kouamé OAAM, Allialy ME** (**2022**). The Geological Formations of Koun Fao (East of Côte d'Ivoire): Petrographic Characterization and Associated Deformations. Open Journal of Geology, vol. 12.

Camil J (**1984**). Pétrographie, chronologie des ensembles archéens et formations associées de la région de Man (Côte d'Ivoire). Implications pour l'histoire géologique du craton ouest-africain. Thèse de doctorat, Université d'Abidjan, Côte d'Ivoire, 306 p.

Coulibaly I (**2018**). Pétrologie des volcanites et des plutonites du sud du sillon birimien de Toumodi-Fetekro (Côte d'Ivoire) : Implications pétrogénétique et tectonique. Thèse de doctorat, Université Felix Houphouet-Boigny, 220 p.

Coulibaly Y, **Boiron MC**, **Cathelineau M, Kouamelan AN** (**2008**). Fluid immiscibility and gold deposition in the Birimian quartz veins of the Angovia deposit (Yaouré, Ivory Coast). , n° 50, pp. 234-254.

Gnanzou A (**2014**). Etude des séries volcano-sédimentaires de la région de Dabakala (Nord-Est de la Côte d'Ivoire) : genèse et évolution magmatique. Contribution à la connaissance de la minéralisation aurifère de Bobosso dans la série de la HauteComoé. Thèse de doctorat, Université Paris-Sud Orsay et Université Felix Houphouet-Boigny, 303 p.

Houssou NN (2013). Etude pétrologique, structurale et métallogénique du gisement aurifère d'Agbahou, Divo, Côte d'Ivoire. Thèse de Doctorat d'Etat, Université Felix Houphouet-Boigny, Abidjan, Cocody, 117 p.
https://earthexplorer.usgs.gov/ USGS website [Accessed 03 February 2024].
Kadio E, **Coulibaly Y**, **Allialy M E**, **Kouamelan A N, Pothin K B K (2010)**. On the occurrence of gold mineralization in southeastern Ivory Coast. Journal of African Earth Sciences, n° 57, pp. 423-430.
Koita M, **Jourde H**, **Ruelland D**, **Koffi K**, **Pistre S, Savane I (2010)**. Cartographie des accidents régionaux et identification de leur rôle dans l'hydrodynamique souterraine en zone de socle. Cas de la région de Dimbokro-Bongouanou (Côte d'Ivoire). Hydrological Sciences Journal, vol. 55, n° 5, pp. 805-820.
Kouadio FJLH (2017). Étude pétro-structurale des formations géologiques du sud-ouest de la Côte d'Ivoire (secteur Bliéron–Grand Béréby) : apport de la géochimie et du couple déformation–métamorphisme. Thèse de doctorat, Université Felix Houphouet-Boigny, Abidjan, Cocody, 221 p.
Kouadio FJLH, Kouamelan, AN, Boya TKL, Kanga RN (2024). Petrographic, Geochemical and Metallogenical Context of the Geological Formations of the Goumere Region (North- East of Cote D'Ivoire): Implication to the Knowledge of Gold Mineralization. Inter national Journal of Geosciences, 15, 180-203. https://doi.org/10.4236/ijg.2024.152012.
Milési JP, **Feybesse JL**, **Ledru P**, **Dommanget A**, **Ouedraogo MF**, **Marcoux E**, **Prost A**, **Vinchon C**, **Sylvain JP**, **Johan V**, **Tegyey V**, **Calvez JY, Lagny P (1989)**. West African deposits in their lower proterozoic lithostructural setting. Chronique de la Recherche Minière, vol. 497, pp. 3-98.
N'Go AY, **Lasm T**, **Koïta M, Savane I (2010)**. Extraction par Télédétection des réseaux de fractures majeures du socle Précambrien de la région de Dimbokro (Centre Est de la Côte d'Ivoire). Revue Télédétection, vol. 9, n° 1, pp. 33-42.
Niamké KH, **Saley MB**, **N'Dri BE**, **Ouattara A, Biémi J (2008)**. Contribution à l'interprétation des linéaments par l'exploitation des pseudo images, de l'hydrographie en région tropicale humide : Cas du N'Zi-Comoé (Centre de la Côte d'Ivoire). European Journal of Scientific Research, vol. 24, n° 1, pp. 74-93.
Oberthür T, **Schmidt MA**, **Vetter U**, **Simon K, Amanor JA (1996)**. Gold mineralization in the Ashanti belt of Ghana : genetic constraints of the stable isotope geochemistry. , vol. 91, n° 2, pp. 289-301.
Ouattara AS, **Coulibaly Y, Kouadio FJLH (2017)**. Les altérations hydrothermales associées à La minéralisation aurifère du gisement de Dougbafla (District d'Oumé-Hiré, Centre-Ouest De La Côte d'Ivoire). European Scientific Journal, vol. 13, pp. 108.
Ouattara G (1998). Structure du batholite de Ferkessédougou (secteur de Zuénoula, Côte d'Ivoire). Implication sur l'interprétation de la géodynamique du paléoprotérozoïque d'Afrique de l'Ouest à 2,1 Ga. Thèse Doctorat ès Sci, Université d'Orléans, 291 p.
Ouattara G, **Gnammytchet BK, Yao KA (2012)**. Contribution des images satellitales Landsat 7 ETM+ à la cartographie lithostructurale du Centre-Est de la Côte d'Ivoire (Afrique de l'Ouest). International Journal of Innovation and Applied Studies, vol. 1, n° 1, pp. 61-75.
Passchier W, Trouw RAJ (1998). Microtectonic., Berlin Heidelberg New York, 229 p.
Perrouty S, **Aillères L**, **Jessell MW**, **Baratoux L**, **Bourassa Y, Crawford B (2012)**. Revised Eburnean geodynamic evolution of the gold-rich southern Ashanti belt, Ghana, with new field and geophysical evidence of pre-Tarkwaian deformations. Precambrian Research, vol. 204-205, pp. 12-39.
Poulsen KH, **Ames DE**, **Lau S, Brisbin WC (1986)**. Preliminary report on the structural setting of gold in the Rice Lake area, Uchi Subprovince, southeastern Manitoba.Natural Resources Canada/CMSS/Information Management geological survey of Canada, n° 86-1B, pp. 213-221.
Sonnendrucker P (1967). Etude de synthèse sur l'or en Côte d'Ivoire. La région aurifère du pays Dida. rapport SODEMI.
Tagini B (1971). Esquisse structurale de la Côte d'Ivoire: Essai de géotechnique régionale., SODEMI, Abidjan.

Téha KR (**2019**). Les formations éburnéennes du sud-ouest du bassin de la comoé et du secteur de singrobo (Sud de la côte d'ivoire) : pétrologie, analyse structurale et magmatisme associé. Thèse de doctorat, Université Felix Houphouet-Boigny, 247 p.
Toutin (**1996**). Opposite Side ERS-1 SAR stereo Mapping over Rolling Topography. Trans. Geosci. Remote Sensing, vol. 34, n° 2, pp. 543-549.
Vidal M, **Delor C**, **Pouclet A**, **Siméon Y, Alric G** (**1996**). Evolution géodynamique de l'Afrique de l'Ouest entre 2,2 Ga et 2 Ga: le style archéan des ceintures vertes et des ensembles sédimentaires birimiens du Nord-Est de la Côte d'Ivoire. Bulletin de la Société géologique de France, vol. 167, n° 3, pp. 307-319.
Yao BD (**1998**). Lithostratigraphie et pétrologie des formations birimiennes de Toumodi-Fettekro (Côte-d'Ivoire): Implication pour l'évolution pour l'évolution crustale du Paléoprotéroïque du craton Ouest-Africain. Thèse de doctorat, Université d'Orléans, France, 191 p.
Yao D, **Delor C**, **Gadou G**, **Kohou P**, **Okou A**, **Konaté S, Diaby I** (**1990**). Notice explicative de la carte géologique de la Côte d'ivoire à 1/200 000, feuille de M'Bahiakro. Mémoire de la Direction des Mines et de la Géologie, n° 2.
Yao D, **Delor C**, **Gadou G**, **Kohou P**, **Okou A**, **Konaté S, Diaby I** (**1995**). Notice explicative de la carte géologique de la Côte d'ivoire à 1/200 000, feuille de Dimbokro. Mémoire de la Direction des Mines et de la Géologie, n° 9, pp. Abidjan, Côte d'Ivoire.